

Transverse-modal behavior of a transverse junction stripe laser excited by a short electrical pulse

Kam Y. Lau and Amnon Yariv

California Institute of Technology, Pasadena, California 91125

(Received 4 August 1980; accepted for publication 29 October 1980)

The transverse-modal behavior of a lateral injection gain-guided laser [the transverse junction stripe (TJS) laser] excited by a short (70 ps) electrical pulse is investigated experimentally and theoretically. It is predicted theoretically and observed experimentally that the transverse mode strongly depends on the excitation pulse amplitude and the dc bias current (which is set below threshold). This dependence is found to be due to transient lateral carrier diffusion at the lasing junction.

PACS numbers: 42.80.Lt, 42.55.Px

Among the many laser structures developed for optical communication, the transverse junction stripe (TJS) laser¹⁻⁴ has established itself as an outstanding candidate—low threshold, high reliability,⁵ flat frequency response⁶—all these are favorable factors for a signal transmitter. Since its inception,¹ significant improvement in performance was made possible by fabricating the laser on semi-insulating substrate,² and recently with MBE-grown layers³ and with a multiple active region having multiwavelength output.⁴ The transient response of this laser, contrary to theoretical predictions, shows little relaxation oscillations. It has been explained with an effective pump rate model, which accounts for both the junction capacitance and the lasing wavelength shift due to heating. The TJS laser has also proven itself capable of generating ultrashort optical pulses (13 ps) by direct-current pulse modulation.⁷ In this paper we present results on the transverse-mode behavior of TJS lasers under short (70 ps) intense electrical pulse excitation. It was experimentally found that the transverse-mode profile depends on the excitation pulse amplitude and, to a lesser extent, on the bias level. The results are successfully explained by theoretical calculations that includes injected carrier diffusion⁸ which significantly affects the gain-guided mode profile. These results are important in high data rate communication links using single-mode fibers, for the transverse-mode pattern of the laser significantly affects the coupling between the laser and the fiber.

A schematic diagram of a TJS laser is shown in Fig. 1. Confined by the heterostructure in the vertical direction, the carriers are injected across the p^+n homojunction in the active layer, thus creating an inverted population near the junction. It has been suggested that¹ the p^+n homojunction actually consists of a p^+pn junction in the parallel direction which provides a builtin index guide, due to a lower refractive index in the highly doped p^+ and n region. The carrier concentrations in the p^+ , p , and n regions are typically 10^{20} , 10^{19} , and $2 \times 10^{18} \text{ cm}^{-3}$, respectively. Recent theoretical and experimental data by Ueno *et al.*¹⁴ show that with these carrier concentrations, index guiding should not be a dominant mechanism. It seems more likely that guiding is provided mainly by the injected holes in the n region. Our experimen-

tal observation that the optical mode actually shifts with injected current density tends to confirm our assumption.

The carrier density distribution $p(x)$ in the steady state takes the form of an exponential extending into the n region:

$$p_0(x) = (\tau/D)^{1/2} J_0 e^{-x/(D\tau)^{1/2}}, \quad (1)$$

where x is the distance measured from the junction into the n side, τ is the recombination lifetime of the carriers, D is the diffusion coefficient, and J_0 is the injection current density. The optical mode guided by a gain distribution given by (1) was found to be a Bessel function of complex order and argument.⁹ The boundary conditions were that the optical field vanishes at $x = 0$ and $x = \infty$. We will use this same boundary condition in solving the transient problem under an injected current pulse.

We shall calculate the time evolution of the optical-mode gain after the injection of an intense narrow current pulse. We assume that the laser is biased way below threshold so that very few photons exist in the cavity. When the current pulse is injected across the junction, the carriers initially accumulate at the junction and do not support a mode with positive gain. Only after the carriers diffuse to a certain width will the mode experience net gain, and an optical pulse follows. The transverse-mode structure of this optical pulse clearly depends on the amplitude and width of the carrier profile at the moment that the mode gain shoots above threshold. Before this moment, we can neglect the optical

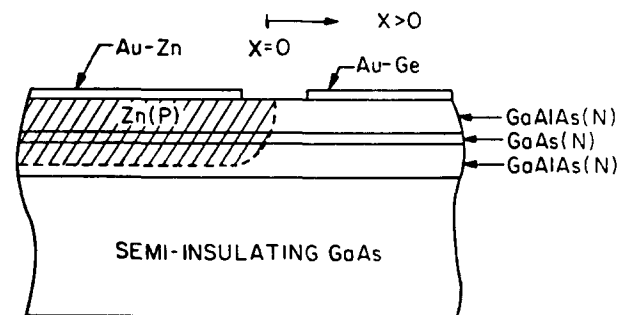


FIG. 1. Schematic diagram of the cross section of a TJS laser.

field and treat the conventional carrier diffusion problem in a straightforward manner.

The transient carrier density distribution satisfies the following field-free diffusion equation:

$$\frac{\partial p}{\partial t} = D \frac{\partial^2 p}{\partial x^2} - \frac{p}{\tau}, \quad (2)$$

where the various variables are defined as before. Suppose that the laser is biased by a dc current and we assume at $t = 0$, a δ -function current pulse of total charge Q is injected across the junction:

$$D \frac{\partial p}{\partial x} \Big|_{x=0} = J_0 + \sigma \delta(t), \quad (3)$$

where $\sigma = Q/wl$, w is the thickness of the active layer, and l is the length of the laser. We assume that before $t = 0$, the system is in equilibrium, i.e., $p(x, t = 0) = p_0(x)$ as given by that in (1). The carrier distribution after $t = 0$ is obtained by solving (2) subject to condition (3), resulting in

$$p(x, t > 0) = \frac{\sigma}{(\pi^{1/2} d(t))} e^{-t/\tau_e - x^2/d^2} + p_0(x), \quad (4)$$

where the time-dependent width of the Gaussian $d(t) = 2(Dt)^{1/2}$. In using (3) as an initial condition, we have assumed that the source impedance of the drive circuit is infinite, i.e., a current source drive. The exact solution in the case of a finite source impedance is highly nonlinear¹¹ and complex. However, it is evident from an equivalent circuit of the laser diode^{6,12} that the above assumption holds for cases where the source impedance is large compared with the diode shunt resistance. This condition, to a fair extent, applies to the actual situation in which the source impedance is 50Ω and the diode shunt resistance is less than 5Ω .

We will next apply the solution $p(x, t)$ of (4) to obtain the transient solution of the electromagnetic laser mode. Since $(Dt)^{1/2} \approx 2 \mu\text{m}$ for $D = 20 \text{ cm}^2/\text{sec}$ and $\tau = 2 \text{ ns}$, we can approximate $p_0(x) = p_0(0) = J_0(\tau/D)^{1/2}$ for the region within 1 or $2 \mu\text{m}$ of the junction. Furthermore, we assume that this carrier profile in (4) produces a gain proportional to the carrier concentration p . The relative permittivity of the medium can thus be written as

$$\epsilon(x) = \epsilon_r + iG [p(x, t) - p_0], \quad (5)$$

where p_0 is the carrier density for transparency, G is the coefficient as defined in (5), which is directly related to the gain coefficient of the laser mode in a straightforward manner, and ϵ_r is the square of the refractive index. With the Gaussian profile in (4) we have

$$\epsilon(x) = \epsilon_r + i(Ae^{-x^2/d^2} - B + C), \quad (6)$$

where $A = G\sigma/[(\pi)^{1/2}d(t)]e^{-t/\tau}$, $B = GP_0$, $C = GJ_0(\tau/D)^{1/2}$. After expanding the Gaussian in power series and keeping the first two terms only, the one-dimensional scalar wave equation with the above permittivity profile reads

$$\frac{d^2 E}{dx^2} + \left(\frac{\omega^2}{c^2} (\epsilon_r + iA - iB + iC) - \beta^2 - \frac{iAx^2\omega^2}{d^2c^2} \right) E = 0, \quad (7)$$

where β is the propagation constant of the mode. This is analogous to the harmonic oscillator, but with an imaginary

quadratic potential instead of a real one.¹⁰ The mode profile, with the boundary conditions $|E| = 0$ at $x = 0$ and $x = \infty$, are therefore the odd parity Hermite-Gaussians

$$E_m(x) = H_m(\alpha x) e^{-1/2\alpha^2 x^2}, \quad (8)$$

where $\alpha = [i\omega^2 A / (c^2 d^2)]^{1/4}$, and with the "energy levels"

$$\frac{\omega^2}{c^2} (\epsilon_r + iA - iB + iC) - \beta_m^2 = (2m + 1) \frac{A}{d} \frac{\omega}{c} e^{i\pi/4}. \quad (9)$$

We are only interested in the lowest-order mode $m = 1$ which is closest to the junction where the quadratic approximation is valid. The maxima of this mode occurs at

$$x_m = \left(\frac{2\lambda}{\pi} \right)^{1/2} d^{3/4} \left(\frac{2}{Ad} \right)^{1/4}. \quad (10)$$

Equation (9) gives the propagation constant β of the mode, and its imaginary part β_i gives the mode gain:

$$\beta_i \approx \frac{1}{2(\epsilon_r)^{1/2}} \left[\frac{2\pi}{\lambda} (A - B + C) - \frac{3}{d} \left(\frac{A}{2} \right)^{1/2} \right]. \quad (11)$$

The product of the width d and the amplitude A of the Gaussian gain profile is, from Eq. (4),

$$Ad = (G\sigma/\sqrt{\pi}) e^{-t/\tau}, \quad (12)$$

so that the mode gain, as a function of time, is

$$\beta_i = \frac{1}{2(\epsilon_r)^{1/2}} \left(\frac{2\pi(G\sigma/\sqrt{\pi}) e^{-t/\tau}}{2\lambda (Dt)^{1/2}} - \frac{3(G\sigma/\sqrt{\pi})^{1/2} e^{-t/2\tau}}{4(Dt)^{3/4}} - \frac{2\pi}{\lambda} (B - C) \right). \quad (13)$$

The first two terms are due to the δ -function current pulse, B is due to intrinsic loss, and C is the contribution from the bias current. The threshold value of β_i for lasing is $(1/l) \ln R$, where l is the length of the laser, and R is the amplitude reflectivity.

We have assumed for convenience in the above calculations that the current pulse is a δ function. In actual experiments, the current pulse is of both finite width and amplitude. In the following numerical calculations, we shall therefore describe the strength of the δ function by an equivalent current amplitude such that a current pulse of this current amplitude and of 70 ps duration (the actual value in our experiments) contains the same amount of charge as in the δ -function pulse. The other parameters we used are $\tau = 2 \text{ ns}$, $G = 6.9 \times 10^{-8} \mu\text{m}^3$, as calculated from Stern's results,¹³ and that the thickness of the active layer is $0.2 \mu\text{m}$ and the cavity length is $250 \mu\text{m}$. The carrier density for transparency is taken to be $2.6 \times 10^{18} \text{ cm}^{-3}$. Figure 2(a) shows a plot of $\beta'_i = \beta_i - [\pi/(\epsilon_r)^{1/2}\lambda] (B - C)$, i.e., the contribution to mode gain due to the current pulse, for various injection pulse strength. We notice that β'_i diverges to ∞ as $t \rightarrow 0$ according to Eq. (13). This is nonphysical and results from the quadratic approximation: at $t = 0$, the carrier distribution is a δ function at the junction, so that in the quadratic approximation it becomes $-\infty$ everywhere except at $x = 0$. An exact numerical solution of the wave equation with the Gaussian profile shows that β'_i actually converges to zero at $t \rightarrow 0$ as shown in Fig. 2(a). This, as mentioned before, results

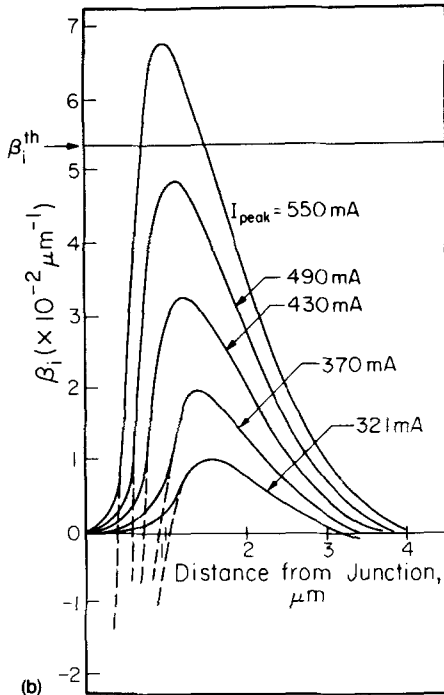
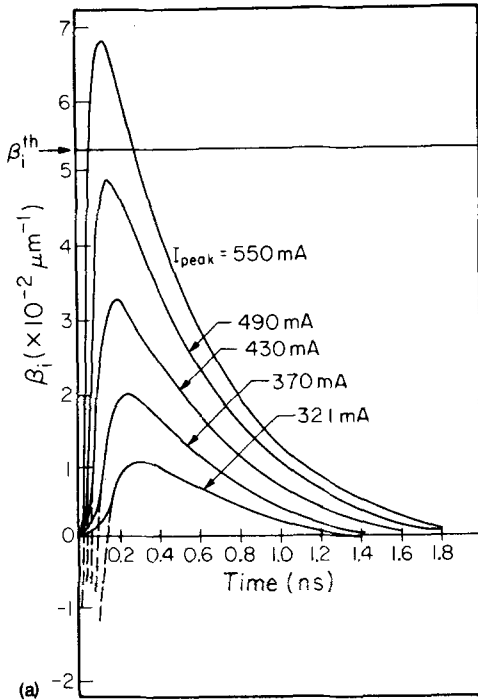


FIG. 2. Plots of mode gain vs (a) time after a current pulse is injected and (b) width of the diffused hole profile in the *N* side of the junction, for various pump current amplitude. β_i^{th} is the minimum mode gain for lasing when no dc bias is applied.

from the fact that a δ -function gain profile does not support a mode with gain. The minimum value of β_i for lasing to occur is

$$\beta_i = \frac{\pi}{\sqrt{(\epsilon_r)^{1/2}} \lambda} (B - C) + \frac{1}{l} \ln R$$

$$= \frac{\pi}{(\epsilon_r)^{1/2} \lambda} G P_0 + \frac{1}{l} \ln R - \frac{G J_0 \pi}{(\epsilon_r)^{1/2} \lambda} \left(\frac{\tau}{D} \right)^{1/2},$$

where J_0 is the dc bias current. The cw threshold current

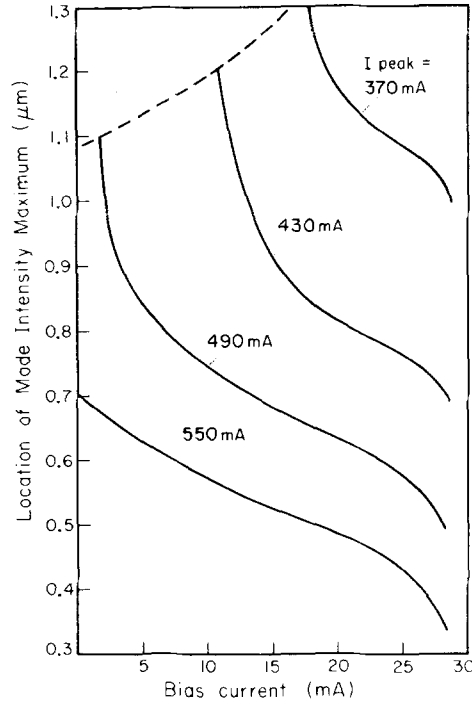


FIG. 3. Plots of positions of the peak of the optical mode at lasing threshold vs dc bias level, for various pump current pulse amplitudes.

calculated with the above parameters is about 30 mA. From Fig. 2(a) we see that the time delay for the mode gain to go above threshold is less for pump pulse of higher amplitude. Since the carrier diffusion distance d and time t are related by $d = 2(Dt)$, we can plot β_i as a function of d , as shown in Fig. 2(b). This plot shows that for a given bias level, at the time lasing occurs, d would be smaller for higher pulse current. The peak of the actual optical mode when lasing first occurs is at a position x_m related to d as in (10). Figure 3 shows a plot of x_m for different bias levels and various pulse current amplitudes.

The dependence of the transverse-mode position on the pulse current amplitude predicted above has been observed experimentally. Figure 4 shows a schematic diagram of the experiment. The laser used was a TJS laser on a semi-insulating substrate with a cw threshold of about 30 mA. The laser was biased with a dc current below threshold, ranging 5–15 mA. It was driven with a step-recovery diode (SRD) which generates 70-ps pulses, of variable amplitude and repetitive at low frequency (250 or 100 MHz). The near field was imaged with a 40 \times , 0.85 NA microscope objective and the

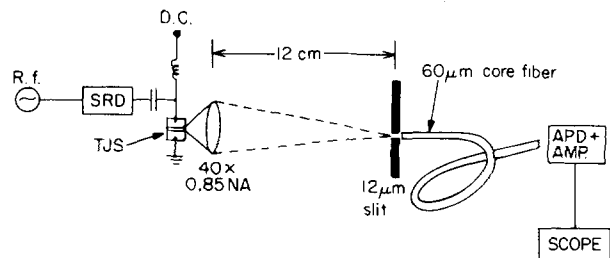


FIG. 4. Schematic diagram of the experimental arrangement for measuring the transient transverse-mode pattern.

time resolved nearfield pattern was measured with a $12\text{-}\mu\text{m}$ slit at the image plane, at a distance of 12 cm from the lens (Fig. 4); the output was detected with a fast rise (100 ps) Avalanche Photodiode (APD) followed by an amplifier, and displaced on a sampling scope. The peak voltage of the pulse output from the step recovery diode is variable between approximately 6 and 15 V (into $50\ \Omega$), which corresponds to peak currents between 200 and 450 mA through the laser. The laser responds to the current pulse with a single sharp optical pulse, the width of which is very possibly below 100 ps—the rise time of the APD used. The transverse-mode structure of this optical pulse is measured by scanning the $12\text{-}\mu\text{m}$ slit along the image plane. It is possible that the transverse-mode structure changes within an optical pulse, but cannot possibly be resolved with the APD.

Figure 5 shows the transverse-mode structure of the optical pulses under different excitation levels. As the peak current of the exciting pulse is increased, the mode shifts closer to the junction. Compared with the mode structure when the laser is operated cw above threshold, the pulsed mode shows a second “bump,” which is possibly the second-order transverse mode. The measurements at different pulse amplitudes are made at different bias levels, for the laser diode cannot be pulsed too high above threshold without destruction. The amount of mode shift measured are in good agreement with theoretical predictions in Fig. 3.

The mode structure of the cw operated laser, contrary to what is expected from theory, does not shift significantly with bias current. This is probably owing to spatial hole burning. At higher bias level, the mode in principle should narrow down and shift toward the junction. Spatial hole burning would, however, counter the above effect and result in a broader mode width than expected. This does not occur in the case of short pulse excitation, because when the photon depletes the gain, the optical pulse is already over. The observed mode shift under pulse excitation, as shown in Fig. 5, just reflects this mechanism.

At a certain fixed bias level, the pump current pulse has to exceed a certain amplitude before an optical pulse is pro-

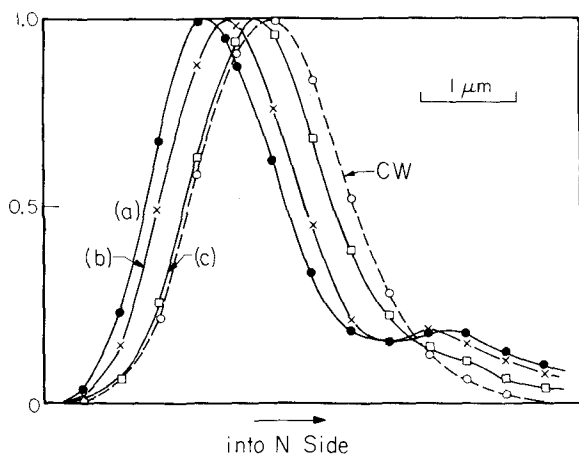


FIG. 5. Measured transverse-mode profile with bias and peak pulse current respectively equal to (a) 12 mA, 430 mA, (b) 15.5 mA, 350 mA, (c) 20 mA, 205 mA. For comparison, the mode profile under cw operation is also shown.

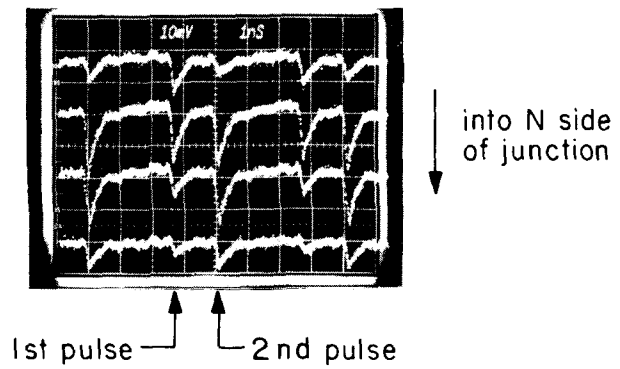


FIG. 6. Output pulses (negative going) from a TJS laser taken at four different positions of the transverse mode, successively going into the *N* side. The laser is excited with two consecutive current pulses, 1.4 ns apart and repetitive at 250 MHz.

duced. At this threshold, the optical pulse has a significant delay, approximately 150–200 ps. When the current pulse amplitude is increased, the delay rapidly shortens and becomes undiscernible. This is also in rough accordance to the calculations of Fig. 2(a). Delays of less than 100 ps, as shown in the figure, cannot possibly be detected by the 100-ps rise-time APD. Moreover, since the current pulse itself is of a finite width of 70 ps, the difference in delay of various pump pulse amplitude might be even smaller than that shown in Fig. 2(a). The transverse-mode position, on the other hand, shows much larger variations than the time delay.

This pump dependence of the transverse-mode structure is strongly manifested when the TJS laser is pulsed by two closely spaced electrical pulses of different amplitude. In our experiment, the second pump pulse is actually due to electrical reflection. The impedance of the laser constitutes a

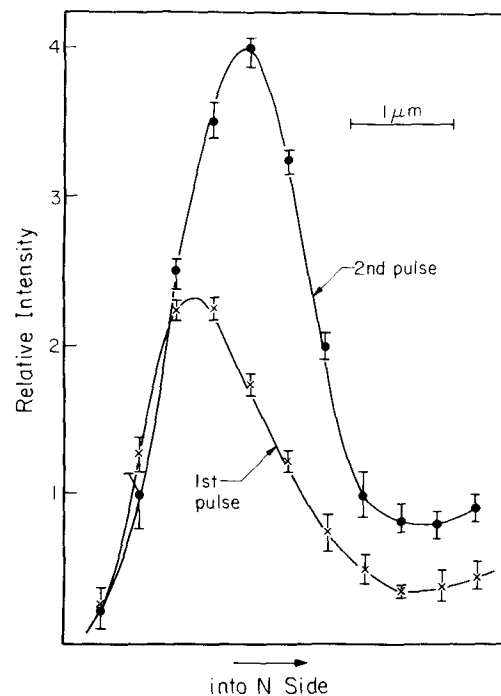


FIG. 7. Transverse-mode profiles of the first and second pulse of Fig. 6.

large mismatch to the $50\text{-}\Omega$ line, and consequently there is a reflected electrical pulse, of about one-half the amplitude of the original pulse and of opposite polarity, propagating from the TJS back to the SRD. The SRD, looking from the output, is a perfect short which then reflects the reflected pulse and inverts its polarity. The separation between these two pump pulses in our experiments is about 1.3 ns, which is comparable to the spontaneous lifetime of the carriers. Even though the second electrical pulse is weaker than the first, the second optical pulse can be equal or even larger than the first one because of charge left over—the pattern effect as shown in Fig. 6. The transverse-mode structure of the two successive optical pulses are distinctively different. As seen from the picture, the *relative* amplitude of the two optical pulses are different when scanned across the transverse-mode profile, which is a clear indication that the mode structure of these two successive pulses are different. Figure 7 shows the transverse-mode pattern of the two pulses. We have performed similar experiments with several other kinds of lasers including proton stripe and CSP lasers, but did not observe the effects described above. Thus it can be concluded that the results are specific to lasers with such a time-dependent gain-induced guiding as the TJS.

Finally, we speculate that the guiding mechanism of the TJS laser is responsible for its ability in generating ultrashort pulses under current modulation. Since the mode is primarily gain guided, the mode loss (or gain) depends crucially on whether the gain profile exists. Because of the short stimulated lifetime, the optical pulses can evolve extremely rapidly (within 10–20 ps) once it breaks above threshold. However, as soon as the optical pulse emerges, the gain is immediately depleted and the guiding no longer exists, resulting in extra-

high mode loss and the optical pulse self-terminates within a few cavity lifetimes. Experimental verification of the above proposition, however, would be very difficult since it calls for measuring the transverse-mode pattern on a ps time scale.

We thank Dr. L. Figueroa and Dr. C. Slayman of Hughes Research Laboratories for helpful discussions as well as supplying the TJS laser used in this experiment. Support of this research by the Air Force Office of Scientific Research is gratefully acknowledged.

- ¹H. Namizaki, IEEE J. Quantum Electron. **QE-11**, 427 (1975).
- ²C. P. Lee, S. Margalit, I. Ury, and A. Yariv, Appl. Phys. Lett. **32**, 410 (1978).
- ³T. P. Lee, C. A. Burrus, and A. Y. Cho, Integrated and Guided-Wave Optics Meeting, Incline Village, January, 1980 (unpublished).
- ⁴W. T. Tsang, Appl. Phys. Lett. **36**, 441 (1980).
- ⁵S. Nita, H. Namizaki, S. Takamiya, and W. Susaki, IEEE J. Quantum Electron. **QE-15**, 1208 (1979).
- ⁶M. Nagano and K. Kasahara, IEEE J. Quantum Electron. **QE-13**, 632 (1977).
- ⁷T. Kobayashi, A. Yoshikawa, A. Morimoto, Y. Aoki, and T. Sueta, Eleventh International Quantum Electronics Conference, Boston, 1980 (unpublished).
- ⁸N. Chinone, K. Aiki, M. Nakamura, and R. Ito, IEEE J. Quantum Electron. **QE-14**, 625 (1978).
- ⁹C. P. Lee, S. Margalit, and A. Yariv, Opt. Commun. **25**, 1 (1978).
- ¹⁰T. L. Paoli, IEEE J. Quantum Electron. **QE-13**, 662 (1977).
- ¹¹B. Lax and S. F. Neustadter, J. Appl. Phys. **25**, 1148 (1954).
- ¹²M. Maeda, K. Nagano, M. Tanaka, and K. Chiba, IEEE Trans. Commun. **COM-26**, 1076 (1978).
- ¹³H. C. Casey and M. B. Panish, *Heterostructure Lasers, Part A* (Academic, New York, 1978).
- ¹⁴M. Ueno and H. Yonezu, J. Appl. Phys. **51**, 2361 (1980).